Industrial Crops & Products 150 (2020) 112421

Contents lists available at ScienceDirect

Industrial Crops & Products

journal homepage: www.elsevier.com/locate/indcrop

Early blight disease management by herbal nanoemulsion in *Solanum lycopersicum* with bio-protective manner

Shipra Pandey[a,c], Ved Prakash Giri[a,d], Ashutosh Tripathi[a,c], Madhuree Kumari[a,c], Shiv Narayan[b,c], Arpita Bhattacharya[a,c], Suchi Srivastava[a,c], Aradhana Mishra[a,c,*]

[a] Division of Microbial Technology, CSIR- National Botanical Research Institute, Lucknow, 226001, India
[b] Plant Physiology Laboratory,CSIR–National Botanical Research Institute, Lucknow, 226001, India
[c] Academy of Scientific and Innovative Research (AcSIR), Ghaziabad, 201002, India
[d] Department of Botany, Lucknow University, Hasanganj, Lucknow 226007, India

ARTICLE INFO

Keywords:
Nanoemulsion
Solanum lycopersicum
Early blight disease
Carbendazim
Plant defence system

ABSTRACT

Early blight, caused by *Alternaria solani* is one of the most devastating disease affecting to the *Solanum lycopersicum* (tomato), reducing its productivity by 80%. The present study illustrates the synthesis of nanoemulsion using peppermint oil for potent antimicrobial activity against *A. solani*. A peppermint oil based nanoemulsion (PNE) was synthesized which was further characterized by Dynamic Light Scattering and Transmission Electron Microscopy. The nano-droplets present in nanoemulsion were spherical in shape with average size < 100 nm. *In-vitro* antimicrobial activity of PNE was examined against *A. solani* with the carbendazim as positive control. A green-house study was performed to evaluate the antimicrobial efficacy and plant immunity developed by nanoemulsion as well as compared with carbendazim, chemical fungicide. PNE was much competent to reduce the disease severity up to 68.7% at 14th day and 87.5% at 21st day respectively. Physiological modulation was showed in tomato plants against *A. solani,* they were confirmed by measured the physical parameters, plant physiology, changes in leaf morphology and stress responses. A significant changes were found in proline and lipid peroxidation content in infected plants whereas nanoemulsion treated infected plants was able to cope-up from stress condition. Physical parameters and Scanning Electron Microscopy (SEM) analysis also revealed the similar observations. A reduced photosynthesis rate and transpiration rate were found in diseased plants as compared to other treatments, although stomatal conductance was not much affected. Defence responsive gene expression also up-regulated in PNE treated diseased plants than pathogen alone. Thus, the current study demonstrated the peppermint oil based nanoemulsion was more efficacious than chemical fungicide to early blight disease management in *Solanum lycopersicum*.

1. Introduction

Productivity of crop is at high risk because of stress conditions; approximately 25% of crop loss was estimated due to pest infestation and diseases (Nicoletto et al., 2019). Though various practices are available to control pests, such as integrated pest management and chemical pesticides, they are not able to overcome the problem in longer term (Oerke, 2006). *Alternaria solani*, causative agent of early blight disease, damaged crop of solanaceae family to a much deeper extent. In *Solanum lycopersicum* (tomato), the productivity loss due to *A. solani* infection was estimated up to 80% (Adhikari et al., 2017). Although, chemical pesticides are commercially available but their prolonged exposure generates multidrug resistance in pathogens, which become environmental and health hazards (Weber and Hahn, 2019; Garnault et al., 2019). In the current scenario, it has become a challenge to investigate a substitute of chemical pesticide to control multidrug resistant phytopathogens in an eco-friendly manner.

In recent decade, nanotechnology has played an important role in agriculture by using nanofertilizer and nanopesticide (Polyakov et al., 2019; Chhipa, 2017). Moreover, various forms of engineered and biologically originated nanomaterials are in use of agriculture but sometime, engineered nanomaterials poses a negative impact to environment (Priester et al., 2012; Raliya et al., 2017). Biogenic nanomaterials have shown antimicrobial activity against myriad of pathogens along with enhanced antimicrobial activity in comparison to engineered and chemically synthesized nanomaterials (Kumari et al (2017 a,b).

* Corresponding author at: Division of Microbial Technology, CSIR- NBRI, Rana Pratap Marg, Lucknow, 226 001, India.
E-mail address: mishra.a@nbri.res.in (A. Mishra).

https://doi.org/10.1016/j.indcrop.2020.112421
Received 30 January 2020; Received in revised form 26 March 2020; Accepted 1 April 2020
Available online 16 April 2020

Application of non-biodegradable nanomaterials is still a big question in agri-sector, urging need of biodegradable nanomaterials to combat the disease caused by phytopathogens. A synergism between crude oil and nanotechnology has resulted into emergence of a new material, introducing the term as nanoemulsion. Nanoemulsion has been used since last decade for various purposes including pharmaceuticals, cosmetics and food industries but in agriculture, it is still at very nascent stage (Araújo al., 2019;Van Tran et al., 2019; Walker et al., 2015). Unlike chemical fungicides and engineered nanomaterials, the green nanoemulsions are biodegradable as well as combat pathogens efficiently (Espitia et al., 2019) in agriculture.

Although a broad range of pesticidal activity of nanoemulsions have been reported against a wide range of insects and microbes (Hashem et al., 2018; Gundewadi et al., 2018), but their action mechanism is still not clearly elucidated. Sharma et al. (2018) demonstrated antifungal activity of clove and lemongrass oil against *Fusarium oxysporum* by disrupting fungal membrane but their effect on plant physiology during host pathogen interaction was not understood completely. Another unique report of antimicrobial activity against food borne pathogens observed by Gundewadi et al. (2018) using basil nanoemulsion compared with carbendazim though the study still leave a lacuna of mechanism.

Peppermint oil, an essential oil obtained from *Mentha piperita* L., profoundly known for their antimicrobial activity (Lim et al., 2018; Benzaid et al., 2019). Although, peppermint nanoemulsion has been reported previously for pesticidal activity (Louni et al., 2018), this is first report as per our knowledge where peppermint based nanoemulsion is being used to control *Alternaria solani* in tomato.

In the present study, role of PNE has been observed against *A. solani* in tomato under green-house conditions. Moreover, the fungicidal activity of PNE has been compared with fungicide carbendazim against *A. solani*. Changes in morphological, physiological, bio-chemical and defence responsive gene expression during tripartite interaction of plant-pathogen and nanoemulsion have been elucidated. Synthesis of peppermint based herbal nanoemulsion for controlling *Alternaria solani*, a substitute of commercially available chemical fungicide is the uniqueness of the study.

2. Materials and Methods

2.1. Materials

All the chemicals used for biochemical assay were purchased from Sigma Aldrich (Sigma Aldrich, India). Peppermint oil used in this study was purchased from HiMedia Laboratories, Mumbai, India. All other reagents used were of analytical grade. A double distilled ultrapure water (18.2 M Ω; Millipore Co., Billerica, MA, USA) was used in the experiments. A tomato variety S-22 used in this study was purchased from the market.

2.2. Synthesis and characterization of PNE

Peppermint oil nanoemulsion (PNE) has been synthesized after preparation of monophasic oil water mixture by following the method of Sugumar et al., 2014. Initially, peppermint oil in concentration of 10% was mixed with 5% of Tween 80 and water was used as an aqueous phase for the nanoemulsion formulation. The mixture was mixed with the magnetic stirrer to make the homogenous solution. Nanoemulsion was synthesized by high energy ultra-sonication method at 30% amplitude, for 20 minutes with 10 sec off and 10 sec on. Further, characterization of synthesized nanoemulsion by following techniques.

2.2.1. Dynamic light Scattering (DLS)

Droplet size distribution frequency was observed by DLS analysis following the method of Guerra-Rosas et al (2016) with some modification. The nanoemulsion was diluted with double distilled water in 1:100 ratio and passed through the 0.45 µm syringe filter. The nanoemulsion solution was used to measure the droplet size and zeta potential of PNE by dynamic light scattering in Zetasizer Nano Series (Nano ZS model ZEN 3600, Malvern, UK) at a fixed scattered angle of 173°.

2.2.2. Transmission Electron Microscopy (TEM)

The TEM analysis was carried out to investigate the accurate and individual droplet size as well as morphology of nanoemulsion, with some modifications in protocol of Silva et al. (2009) and Nam et al. (2012). Nanoemulsion samples were sonicated for 2 minutes before grid preparation. After sonication, a drop of nanoemulsion was placed on foamwar coated copper grid and left overnight to complete dry. Samples were negatively stained with the 2% (w/v) of uranyl acetate and allowed to dry for one hour, then observed under the TEM at 80 KV (Technai 1321 G2 Spirit, TWIN, USA).

2.3. In-vitro antimicrobial activity of PNE against Alternaria solani

2.3.1. Agar diffusion assay

Potato dextrose agar (PDA) plates were supplemented with different concentrations viz. 0.25, 0.5, 0.75 and 1% of PNE separately. A 4 mm fungal bid (*A. solani)* was kept at the center of the plate to study the antifungal efficacy and minimum inhibitory dose of PNE. The antifungal efficacy was measured by comparing the growth of pathogen in control plate (without any treatment) and expressed in terms of percent inhibition. To evaluate the enhanced activity of PNE, a comparative antifungal activity also observed between peppermint crude oil and nanoemulsion. PDA plates were supplemented with 1% of PNE, another set of plates were prepared by supplemented with crude oil; the amount of crude oil was inoculated as equivalent to oil present in 1% PNE. Plates were used without treatment served as control. Thereafter, fungal bid was kept at the center of the plates and incubated for seven days to observed the antifungal activity.

2.3.2. Broth assay

Potato dextrose broth (PDB) was prepared by supplemented with different concentrations viz; 0.5, 0.75 and 1% of PNE. Two fungal bid were inoculated into the medium that carried 5×10^4 spores/mL. On day seven, fungal mycelia was filtered and kept at 45 °C for 48 h, thereafter biomass was measured and calculated the percent inhibition as compared with control.

2.4. Dose determination of nanoemulsion by leaf detached assay

To assess the vital dose of PNE, 15 days old leaves were used for the experiment. Leaves were washed thoroughly with distilled water, followed by 30 sec treatment of 0.1% Sodium hypochlorite and washed with sterile distilled water. Thereafter, leaves were treated with 70% ethanol for 5 min, rinsed thrice with distilled water. After adequate sterilization, leaves were dipped into different concentration of PNE (0.25, 0.5, 0.75, 1, 5 and 10%) for 10 min, control leaves were dipped into sterile distilled water. All treated leaves were placed on 0.8 % agar plates, left it for 10 min till become dry. Spore suspension of *A. solani* was prepared in 1% gelatin with spore count 10^6 spores/mL. Two drops of 10 µl of spores suspension was spotted on each treated leaves and plates were incubated at 28 °C for five days.

2.5. Green-house studies

The greenhouse experiment was set up by the following method of Dixit et al. (2016) with some modifications. Tomato seeds (S-22) were sown in garden soil and kept at 25 °C in dark condition. After the germination of seeds, seedlings were kept in greenhouse conditions (28 °C/22 °C day/night and 62% relative humidity). Four weeks old tomato seedlings were transplanted into 10 inch plastic pots containing garden

soil and categorized in six groups. **1**. Control (Con) **2**. 1% PNE (PNE) **3**. 0.1% carbendazim (carb.) **4**. *A. solani* (AS alone) **5**. PNE with *A. solani* (AS + PNE) **6**. Carbendazim with *A. solani* (AS + Carb). Control plants were sprayed with 1% gelatin, whereas PNE and carbendazim were sprayed on plants with 1% and 0.1% concentration respectively. After two hours from the treatments of PNE and Carb on AS + PNE and AS + Carb subjected plants, the spore suspension of *A. solani* (10^6 spores/mL) was applied on AS, AS + PNE, AS + Carb and AS alone. Plants were bagged with transparent plastic bag to maintain the moisture for 48 h. After 48-72 hours, plastic bags were removed and plants opened in greenhouse condition till the harvesting.

2.6. Disease assessment parameter

Fresh samples of tomato leaves were collected at day 7, 14 and 21 from all the treatments for the assessment of disease severity in leaf by *A. solani*. The tomato leaves were crushed in double distilled water and the sap was centrifuged at 5,000 rpm for 5 min. 10 µl of supernatant dropped on hemo-cytometer and spores were counted and calculated per mL of sap.

2.7. Assessment of physical parameters

Physical parameters of plants were assessed by measuring their root length, shoot length, fresh and dry weight. For dry weight, after measuring the fresh weight whole plant was kept at 50 °C for 72 h in oven, after that the dry weight of the plant was measured. The chlorophyll content was determined as followed the method of Arnon (1949).

2.8. Stomata Morphology

For evaluation of morphological anomaly in tomato leaves after pathogen infection, scanning electron microscopy (SEM) was carried out with some modification in protocol of Tiwari et al. (2014). After 72 h of infection, tomato leaves were plucked from each treatments: control, AS, AS + Carb and AS + PNE. The leaves of tomato were cut into 5 mm^2 pieces and fixed immediately into 4% formaldehyde and 2% glutaraldehyde with cacodylate buffer 0.1 M, pH 6.9. After 24 hr, the samples were rinsed in 0.1 M cacodylate buffer and fixed in 1% osmium tetroxide in cacodylate buffer pH 6.9 for 2 h at 4 °C. The pieces were dehydrated in alcohol series from 10% to absolute alcohol. Furthermore, fixed and dehydrated samples were dried by critical point method. The samples were spur coated by gold metal (Sputter Coater Q150TES, High vacuum coating unit) and analyzed in high vacuum mode at high resolution field emission E.M., Quanta SEM field emission gun (Quanta 250 FEG, FEI).

2.9. Stress parameters

2.9.1. Proline

Total proline content in tomato leaves was determined by following the method of Bates et al. (1973) with some modification. Briefly, leaf tissue (100 mg) were homogenized with 3% sulphosalycylic acid. One ml supernatant of homogenized mixture was mixed in 1 mL of glacial acetic acid and 1 mL of ninhydin reagent, mixture was boiled at 100 °C for 30 min. Two phase was separated after cooling, the absorbance was measured at 520 nm by spectrophotometer of chromophore containing toluene layer.

2.9.2. Lipid peroxidation

Lipid peroxidation (LPx) was estimated by thiobarbituric acid as a reactive substance (TBARS) content by following the method of Heath and Packer (1968) with some modification. In brief, 100 mg of leaves tissues were homogenized with 0.1% Tricholro acetic acid (TCA) and mixture was centrifuged at 5,000 rpm for 5 min. 20 % of TCA containing 0.5% thiobarbituric acid mixed with 1 mL of supernatant of sap and boiled at 95 °C for 30 min. After heating samples were transferred immediately in ice and absorbance was recorded at 532 and 600 nm.

2.9.3. Phenylalanine ammonia-lyase (PAL)

For estimation of PAL activity, firstly a leaf extract was prepared by following the method of Kumari et al. (2017b). Before measuring the PAL activity, total protein content was assessed by Bradford method (1976). Thereafter, 1 mL reaction mixture was prepared by mixing 100 µl of extract, 900 µl of 6 µM L-phenylalanine and 0.5 M Tris-HCl buffer solution. Following mixture was kept at 37 °C for 70 min in water bath. PAL activity was measured at 290 nm by spectrophotometer and expressed as µM TCA/g of protein.

2.10. Assessment of physiological parameters

Changes at physiological level in tomato leaves were assessed by examined the rate of transpiration, rate of photosynthesis, stomatal conductance and water use efficiency (WUE) by using a portable photosynthetic gas exchange system (Li-6800, LI-COR, Lincoln, USA). During observations, photosynthetic photon flux density was maintained at 790-800 µmol m^{-2} s^{-1} with 23-25 °C air temperature, whereas the leaf temperature of tomato was 21-25 °C. The average relative humidity of surroundings (61.96 %) and internal CO_2 was ~320-400 µmol mol^{-1} with ambient CO_2 ~400-490 µmol mol^{-1}. All the observations were performed with three biological as well as five technical replicates.

2.11. Quantitative real time PCR analysis of defense responsive genes

Total RNA was extracted from all the treatments after 48 h post infection by using RNA extraction kit (Sigma, USA), following the given protocol, in RNase free condition. The concentration of RNA was determined by Nano Drop (Thermo Fisher Scientific, USA). Furthermore, 1 µg of RNA was used for cDNA synthesis by using Maxima First Strand cDNA Synthesis Kit (Thermo Scientific, USA) as per manufacturer's instructions. Synthesized cDNA was diluted with nuclease free water in ratio of 1:5. A quantitative RT-PCR was carried out after mixing 1 µl of cDNA with 5.0 µl of Brilliant III Ultra-Fast SyBR® Green (QPCR master Mix Agilent Technologies, USA) and 1.0 µl of primer (10 pmol forward/reverse), maintained the final volume 10 µl, in Strata gene Mx3005 P instrument (Agilent Technologies, USA). A total 5 primer set was designed for cDNA (except *Actin*) by Kegg database and retrieved from National Centre for Biotechnology (NCBI) database. List of primer was given in Table 1. *Actin* gene was served as an internal reference. Conditions for the thermal cycling was as follows: initial denaturation at 95 °C for 15 min, the second segment denaturation at 95 °C for 10 s, primer annealing (30 s at 55-58 °C as mentioned in Table 1 for specific primer) and extension (30 s at 72 °C) for 40 cycles followed by dissociation segment. The final step was melting curve programme (95 °C for one min). The threshold cycle (C_T) was used to represent the relative mRNA amounts in fold change. All samples were run and analyzed in calculated in $2^{-\Delta\Delta C\ T}$(Livak and Schmittgen, 2001) and expressed in fold change.

2.12. Statistical analysis

All the experiments were performed at least three times and represented in terms of means ± SE in histograms. SPSS software was used for the each experiment, represented by different alphabets according to Duncan's multiple comparison test ($P < 0.05$)

3. Result and discussion

3.1. Synthesis and characterization of PNE

The PNE was synthesized by high energy method, using

Table 1
List of primers used for the study of changes at gene expression level in tomato during interaction of different treatments: Control, Carb, PNE, AS, AS + Carb and AS + PNE.

S. No.	Gene name	Sequence (3'-5' F/R)	Gene ID	Annealing Temperature
1	*NHO1*	F-TGGATGCACGTACCAGTTCT R-CCTTCTCCACACCTCCTGTT	XM_004235853.4	56°C
2	*NPR1*	F-CCGCGGACTAGTACTACCAG R-GATCTAGCGGCTGAGAGTGT	XM_004249185.4	58°C
3	*PR1*	F-GCCTTTGCCCAAAATTACGC R-ACAACCAAGACGTACCGAGT	LOC100191111	55°C
4	*WRKY-31*	F-GACCTATGGCACCGACCATA R-GGCTCGTCCTTAGTTCTCGA	NM_001319981.1	56°C
5	*MYC2*	F-TTTGGCAATCGTCGGTTGTT R-CATCAACCGCATCATCCGTT	NM_001324483.1	56°C

ultrasonicator, a probe having piezoelectric crystal, generates cavitation force under high pressure (McClements, 2011) to breakdown the big oil droplet into smaller ones. Moreover, ultrasonic method requires less surfactant and gives more stability, hence the method is more efficient than others (Walia et al., 2017). Nanoemulsion formulation contains ten percent of peppermint oil. Furthermore, their effective doses (0.5, 0.75 and 1%) for growth inhibition of *A. solani* was evaluated by minimum inhibitory concentration.

Droplet size of nanoemulsion is utmost defining factor that significantly affect the antimicrobial efficacy against pathogens. Size distribution frequency of nanoemulsion measured by DLS was < 100 nm whereas zeta (ζ) potential (ZP) denoting surface charge of PNE was negative charged (-16.2 ± 0.20) supported to long term stability of the droplets (Fig. 1 c, d).

The accurate size and morphological feature of droplet was observed under TEM. The size of PNE droplets were determined in the range of 20-40 nm (Fig. 1b). Nevertheless, type of surfactant plays major role in determining the size of the droplets. A study of Saberi et al., 2013 highlighted that the smallest droplets were present in the system using Tween 80 surfactant as compared to other Tween group. Similar observation was found in study of Ostertag et al. (2012), the findings were focused on synthesis of nanoemulsion having smaller droplet in low concentration of Tween 80.

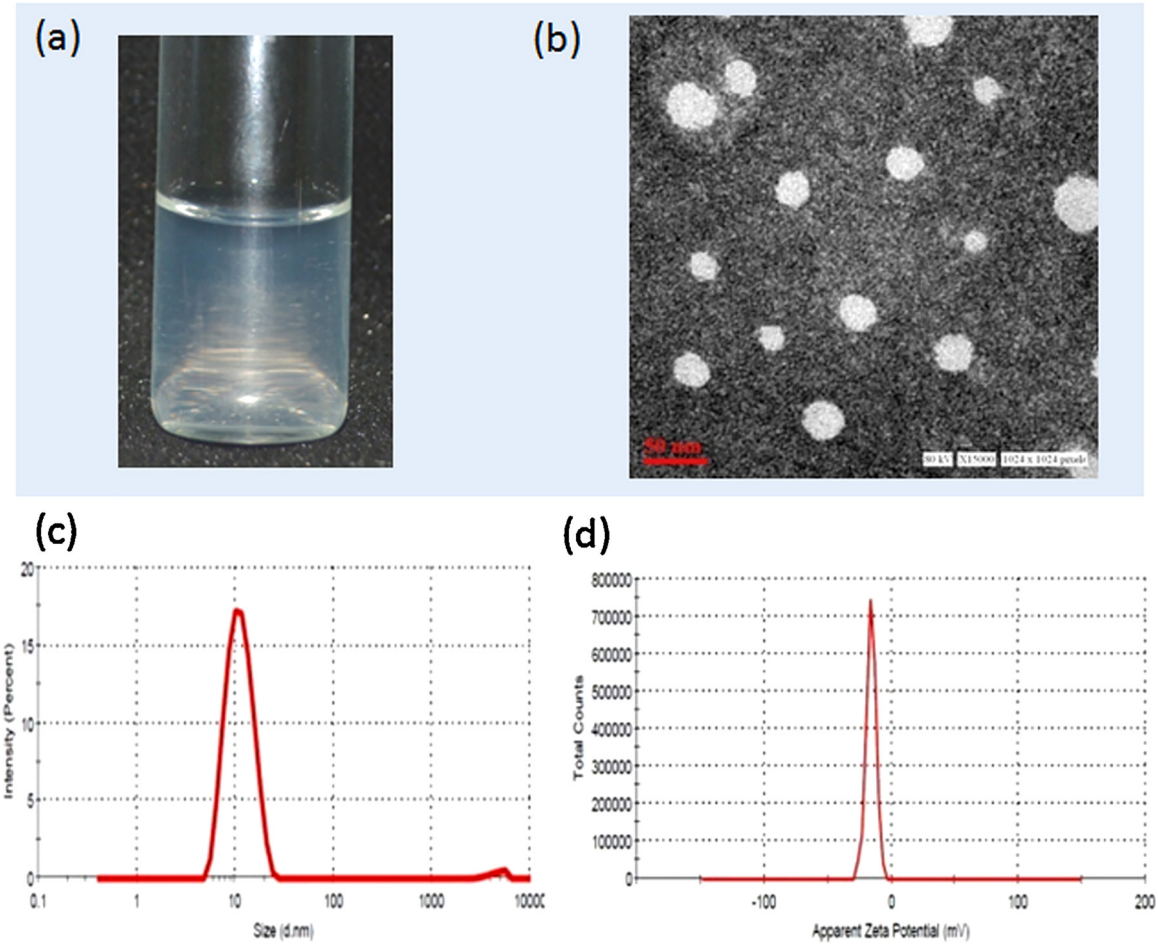

Fig. 1. One percent Peppermint oil based nanoemulsion (a) and its characterization by TEM micrograph (b) hydrodynamic size distribution of PNE (c) and zeta potential (d).

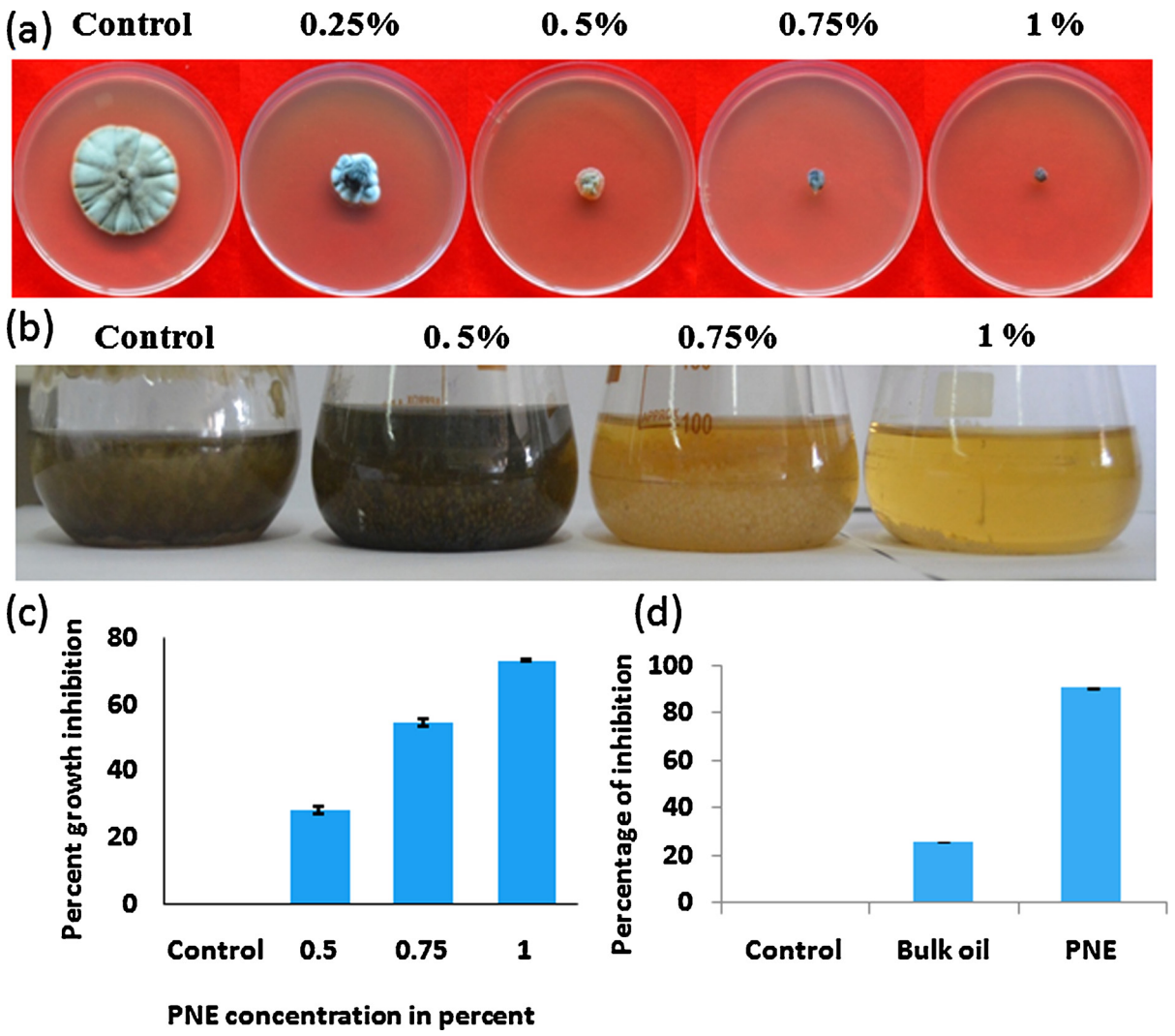

Fig. 2. Evaluation of antimicrobial efficacy of PNE against *A. solani* by agar diffusion assay (a) and broth assay (b) percent growth inhibition by biomass reduction (c) and comparative study of antimicrobial efficacy of peppermint oil and PNE (d).

3.2. Antimicrobial activity of PNE against A. solani

Antimicrobial property of PNE was evaluated against *A. solani*. In agar diffusion assay, 0.25 % dose of PNE showed growth inhibition which further enhanced with higher concentrations of PNE (Fig. 2a). Whereas, in broth assay, biomass of *A. solani* at different concentrations viz. 0.5, 0.75 and 1% were reduced by 28, 54 and 73 % respectively (Fig. 2b, c). One percent of PNE showed maximum biomass reduction in *A. solani* (Fig. 2c). A comparative antifungal activity against *A. solani* was also performed to evaluate the potential of 1 % PNE and bulk peppermint oil. Enhanced activity was observed in PNE as compared to bulk oil activity. A 90 % inhibition was observed in PNE, whereas bulk oil showed up to 26 % inhibition. Therefore, 64% enhanced activity was observed (Fig. 2d). There may be myriad of reasons for potent antimicrobial activity of PNE. It might be greatly affected by the size and shape of the droplet and antimicrobial compounds of oil. Moreover, small droplet size having increased surface area can be enhance the interaction with pathogen showing maximum antimicrobial activity (Kumari et al., 2017a). Peppermint oil has been reported previously as potential antimicrobial agent due to presence of menthol, menthone, 1,8 cineole, caryophyllene etc (Khan and Abourashed, 2011; Mahboubi and Kazempour, 2014). A recent study of Liang et al. (2012) also compared the antimicrobial activity of peppermint oil and its nanoemulsion against food pathogens, they have observed that minimum inhibitory concentration of bulk oil and nanoemulsion were same, nonetheless NE was more effective due to long term inhibition.

3.3. Dose determination of PNE by detached leaf assay

In-vitro study of PNE with *A. solani* was done to determine the potent dose of nanoemulsion (0.5-10%) for foliar spray on tomato plants during early blight disease management. In detached leaf assay, the tomato leaves was observed at day 3, 0.5 to 2.5% PNE were sufficient to inhibit the growth and infection of *A. solani* spores. Moreover, without PNE treated leaves, spores of *A. solani* had started infection and conidia formation resulting chlorosis of the leaves, which was gradually increased by further incubation up to 5th day (Fig. 3 a, b). It was also recorded that at 5th day, 0.5 and 0.75% PNE treated tomato leaves showed infection. Though the increased dose of PNE i.e. 2.5, 5 and 10 % were able to inhibit the growth of pathogen but did not show any positive effect on plant health as data recorded on 5th day, there is might be the possibly the over dose of PNE (Fig. 3 b). Findings of detached leaves assay highlighted the 1% PNE showed an inhibitory effect of *A. solani* without a negative effect on tomato leaves. Results were corroborated with the previous finding of Kumari et al. (2017) during pretreatment of biogenic silver nanoparticles on tomato leaves for the prevention of *A. solani*.

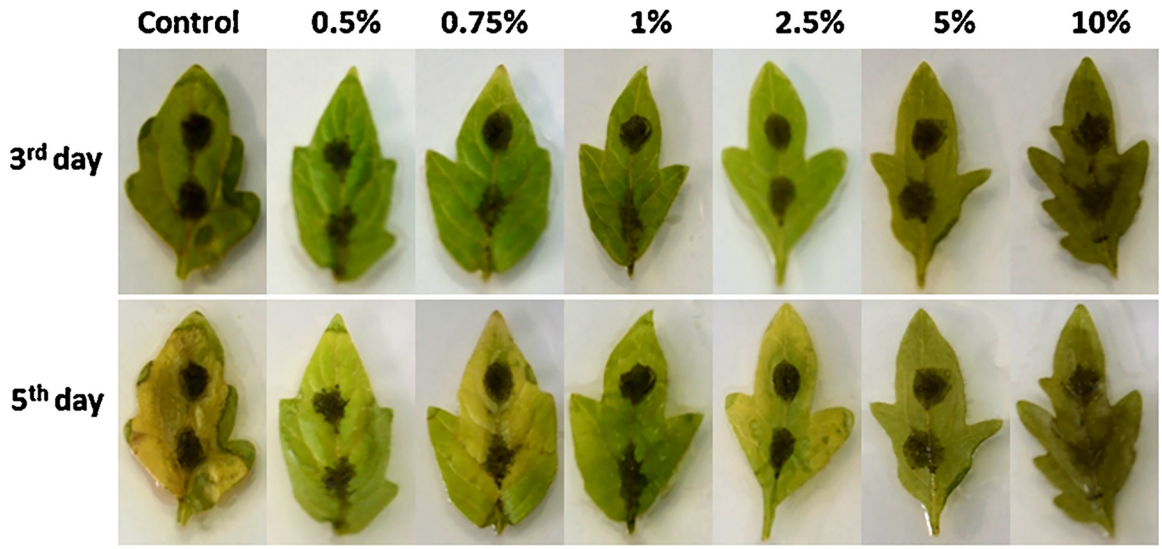

Fig. 3. Detached leaf assay of tomato leaves treated with different doses of PNE (0.5, 0.75, 1, 2.5, 5, and 10%) at 3rd and 5th day.

3.4. Greenhouse experiments

A green-house experiment was carried out to evaluate the antimicrobial efficacy of PNE against *A. solani*, the causative agent of early blight disease in tomato (Fig. 4a). After 72 hours of post infection, symptoms were appeared on *A. solani* infected treatments and it was noted that 1% PNE exhibited a strong antifungal activity in AS + PNE treatment. Although, 0.1% Carb also able to inhibit the fungal growth in AS + Carb (Fig. 4b). The similar results were reflected in spore count also, the spores were found at 7th day in pathogen infected (AS alone) plant only, and it was increased with the time, at 14th and 21st day. In other treatments, no symptoms were found at 7th day, while spore count was decreased up to 31.2 and 54.5 % at 14th and 21st day respectively in AS + Carb treated plants. Whereas, AS + PNE was much competent to reduce the disease severity up to 68.7% at 14th day and 87.5% at 21st day (Fig. 4c). These plausible observations clearly indicated that disease severity is dependent on the spore density in leaf. During necrophytic infection, inoculums of spores triggers plant immune response resulting cell death in higher spore density area (Pétriacq et al., 2016).

Extension of investigation proceeded towards physical parameters measured by root length, shoot length, biomass of the plant. Shoot length of compromised plants (AS alone) were reduced up to 16.5% as

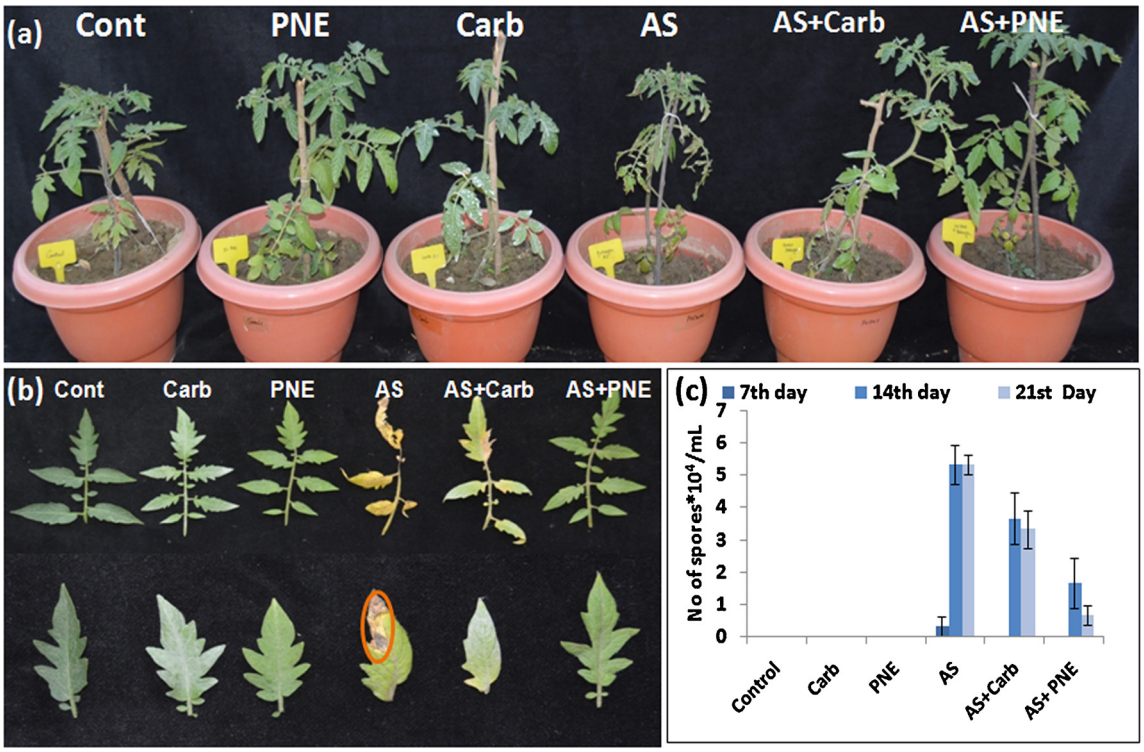

Fig. 4. Greenhouse experiment for evaluation of antifungal activity of PNE herbal nanoemulsion against *A. solani* in tomato. Six treatment were selected for the experiment: Control (negative control), Carb (Carbendazim: chemical fungicide only), PNE (PNE nanoemulsion treatment only), AS (*A. solani* pathogen only), AS + Carb (Carbendazim with pathogen), AS + PNE (PNE nanoemulsion with pathogen) (a) Visually appearance of disease symptoms in tomato leaves (b) Reduction in spore count at day 7, 14 and 21 (c).

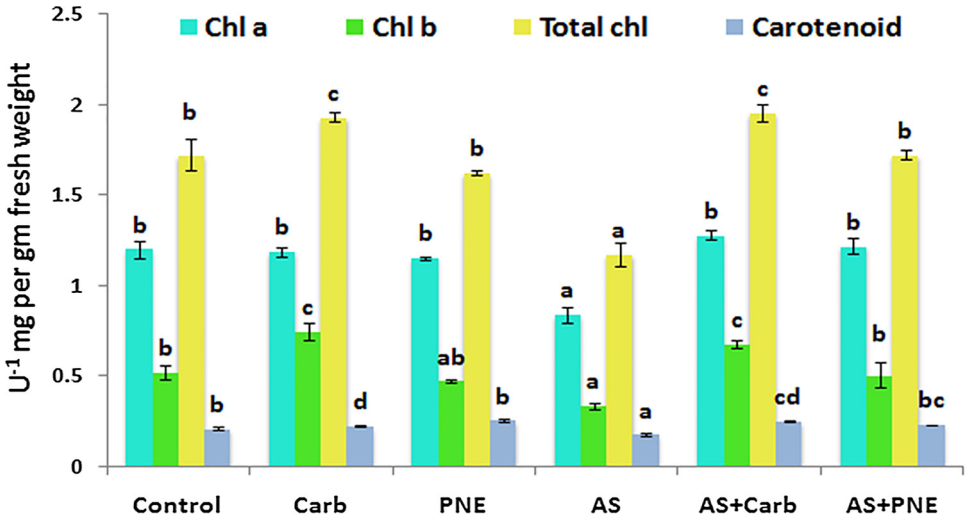

Fig. 5. Chlorophyll and carotenoid content in different treatments: Control, Carb, PNE, AS, AS + Carb and AS + PNE. Significantly difference was determined by SPSS and different alphabets represented according to Duncan's multiple comparison test ($P < 0.05$).

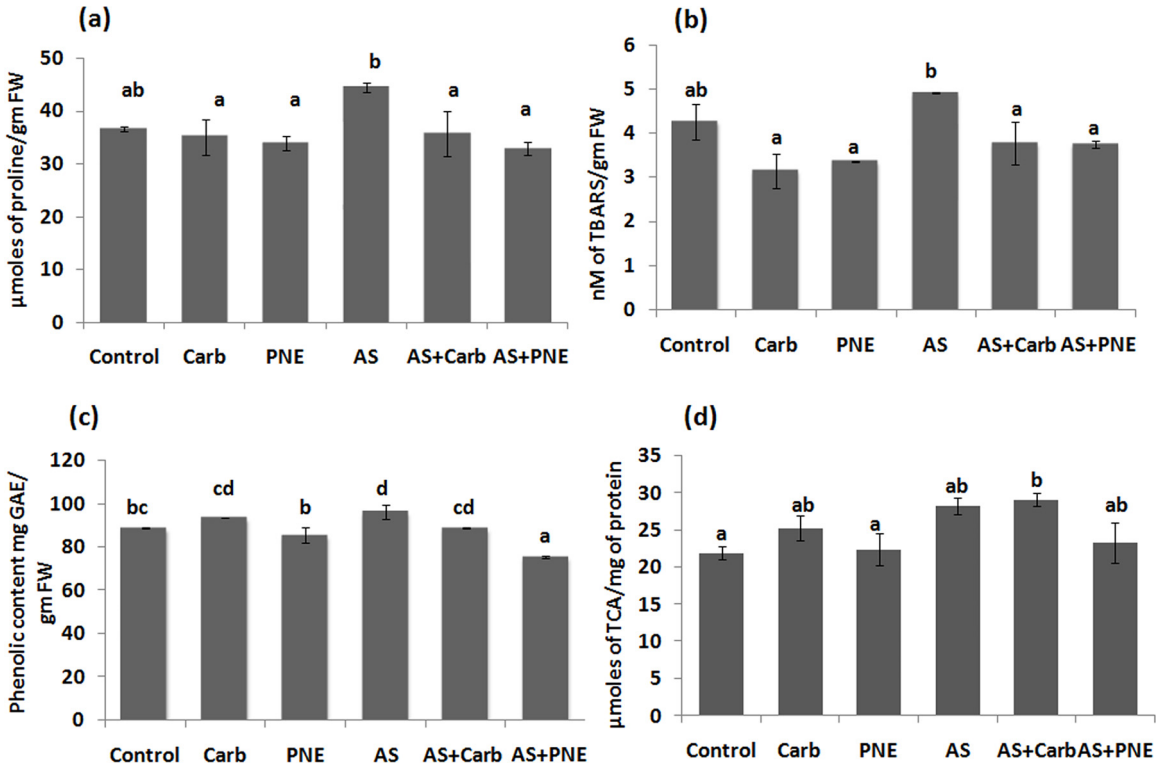

Fig. 6. Assessment of non-enzymatic and enzymatic activity in tomato leaves treated with different treatments: Control, Carb, PNE, AS, AS + Carb and AS + PNE; by estimation of proline (a), lipid peroxidation (b) and total phenolic content (c) Phenylalanine ammonia-lyase (d). Significantly difference was determined by SPSS and different alphabets represented according to Duncan's multiple comparison test ($P < 0.05$).

compared with control while AS + Carb and AS + PNE treated plants enhanced significantly by 10.4% and 9.19% respectively than compromised plant (Fig S1 a). In contrast, root length of AS infected plants were decreased in respect to control plants, while AS + Carb and AS + PNE treated plants were also reduced the root length in comparison to control and pathogen infected plants (Fig S1 b). These results indicating the possibility of plant stress amelioration by biomass conservation process in chemical fungicide (AS + Carb) and PNE (AS + PNE) treated pathogen infected plants.

Similarly, dry weight of pathogen infected plants decreased in comparison to control plants, while AS + PNE and AS + Carb treated plant dry weight was enhanced but it was not significantly distinct than pathogen infected plants (Fig S1 c, d). There were also a significant difference found in plant cholorophyll content (Fig. 5). A 30.2 % and 35.5% cholorophyll "a" and "b" reduction was estimated in pathogen infected plants, while Chl "a" and "b" were enhanced in AS + Carb (34.3, 35.2%) and AS + PNE (31.1, 33.5%) treated plants, than compromised plant (AS alone). Similar observation was found with carotenoid content in tomato leaves (Fig. 5). A previous report also has been found the pathogenic infection directly affected to the plant physiology by reducing chlorophyll content in compromised plant than un-infected plants. Likewise, Dallagnol et al. (2011) revealed that a reduced content of chlorophyll was observed in pathogen infected plant which is simultaneously affecting the photosynthesis rate also.

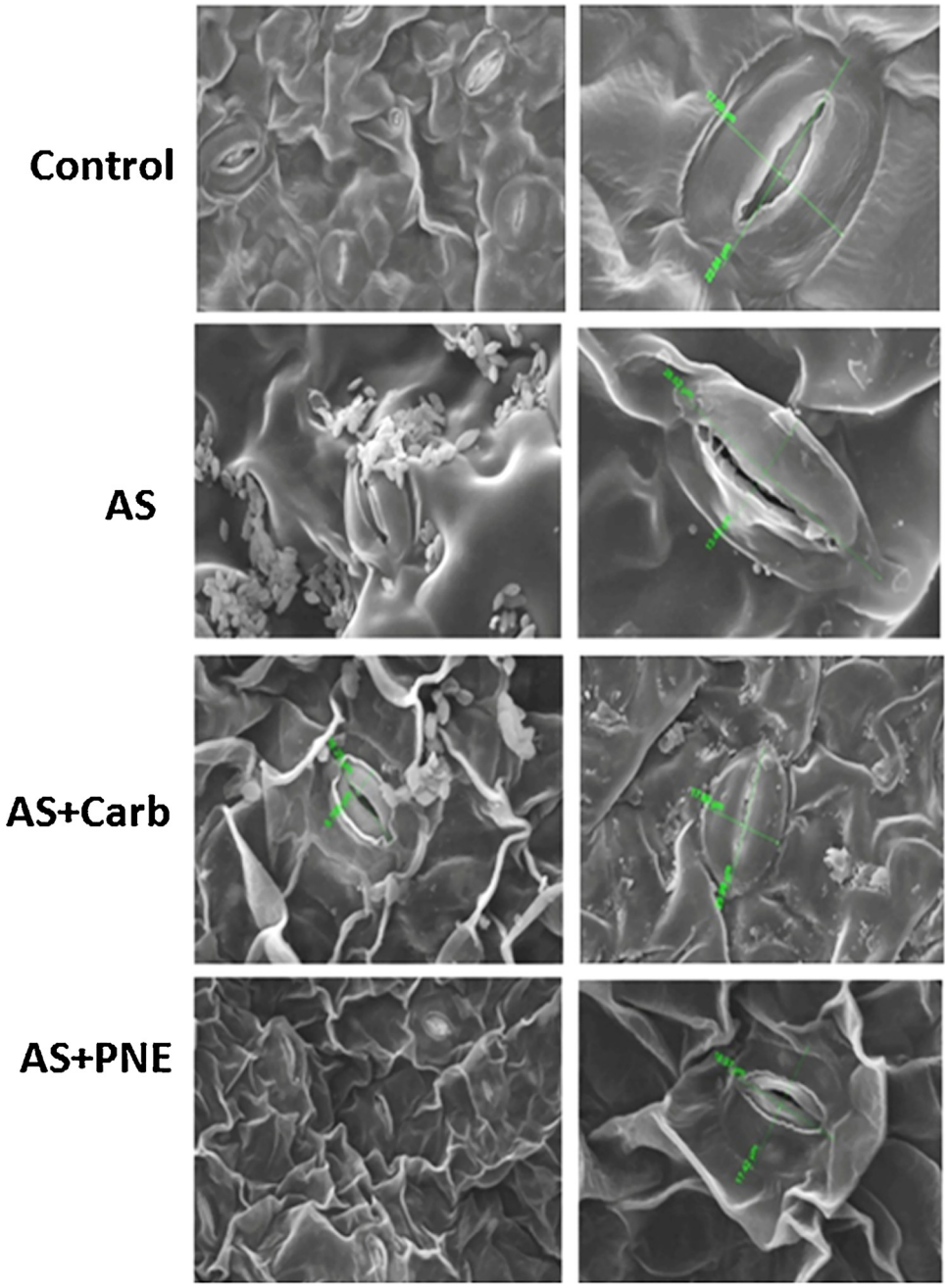

Fig. 7. Scanning electron micrographs of tomato leaves (adaxial surface) during interactions with different treatments: Control, Carb, PNE, AS, AS + Carb and AS + PNE at higher magnifications.

3.5. Assessment of stress parameters and enzymatic activity during infection

To assess the level of stress, major stress markers were observed by proline and lipid peroxidation content in all the treatments. Proline and LPx are considered as primary stress markers during biotic stress (Kumari et al., 2017a, Lopisso et al., 2017). Accumulation of proline content was higher by 44.38 µmoles of proline/gm FW in pathogen infected plants (AS alone) indicating the higher stress condition. Whereas, lower proline accumulation was observed in pathogen infected plants treated with PNE (32.83 µmoles of proline/gm FW) and carbendazim (35.69 µmoles of proline/gm FW) than AS alone and control plants (Fig. 6a). Likewise, LPx content was also increased in pathogen infected plants by 4.9 nM of TBARS/gm FW, however decreased LPx activity by 3.74 nM of TBARS in PNE treated pathogen infected plants, indicated the healthier condition than infected plants (Fig. 6b). AS + Carb treated plants were also able to lower the stress condition which was nearly equivalent to AS + PNE treated plants. Proline is a low molecular weight compound, acts as an osmo-regulator, plays key role in osmotic balance and prevents cell organelle from oxidative damage (Vendruscolo et al., 2007; Jain et al., 2001). A study of Aswani et al. (2019) reported that Pyrroline-5-carboxylate synthetase (P5CS, involved in biosynthesis of proline) and proline dehydrogenase (PDH, involved in oxidation of proline) enzymes regulates proline metabolism. During oxidative stress condition up-regulation of P5CS and down regulation of PDH resulted in enhanced proline accumulation during oxidative stress (Aswani et al., 2019). Moreover, malondialdehyde (MDA) content, is a marker of lipid peroxidation in membrane of tissue enhanced during stress condition (Zhao et al., 2012; Meena et al., 2016). A similar finding was observed by Lubaina and Murugan (2013), where MDA content was enhanced in *Sesamum*

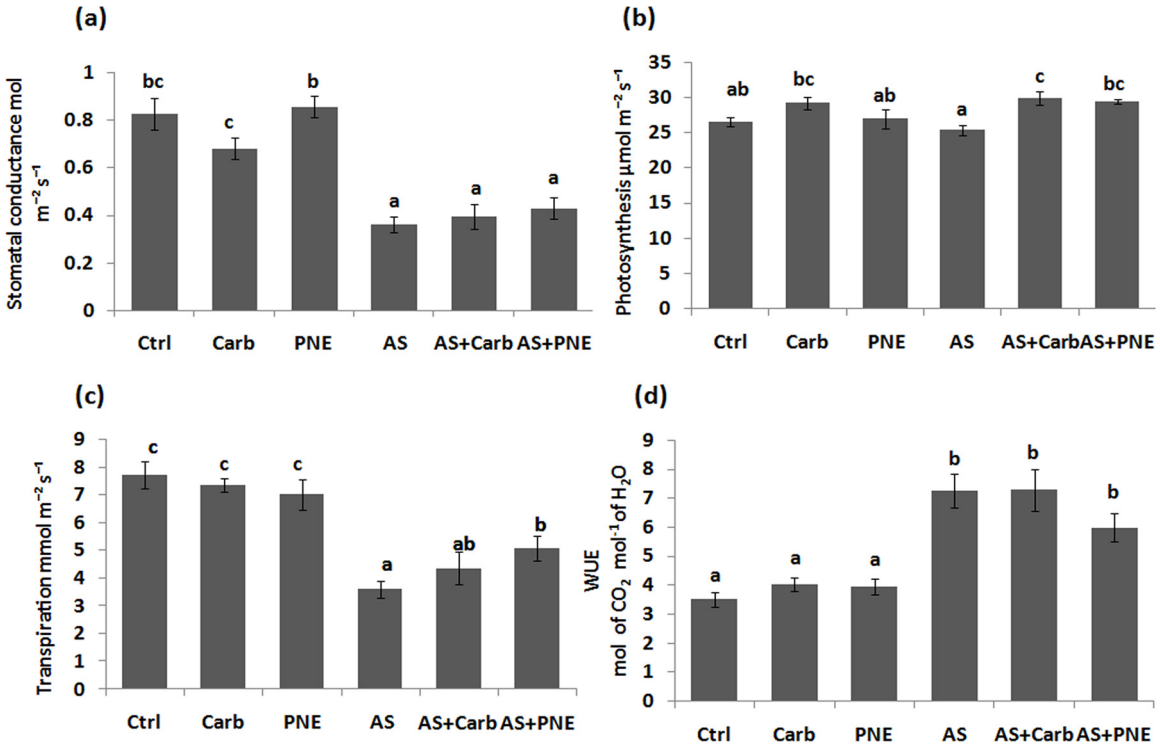

Fig. 8. Changes in physiology of tomato leaves during interaction with different treatments: Control, Carb, PNE, AS, AS + Carb and AS + PNE; by stomatal conductance (a) rate of photosynthesis (b) rate of transpiration (c) and water use efficiency (d). Significantly difference was determined by SPSS and different alphabets represented according to Duncan's multiple comparison test ($P < 0.05$).

orientale after infection of *Alternaria sesami*. Free radicals generates during stress condition in plants, resulting enhance toxicity in cell (Jaleel et al., 2009). Plants respond to scavenge these free radicals by producing antioxidant compounds (Singh et al., 2013).

Furthermore, total phenolic contents were maximum recorded in AS alone 96.92 mg GAE/gm FW of infected leaves after 72 h of post-infection, whereas minimum accumulation was found in AS + PNE (75.52 mg GAE/gmFW) which was significantly less than control (88.7 mg GAE/gm FW) (Fig. 6c). Non-enzymatic stress parameter such as phenolic compounds, a metabolite of phenylpropanoid biosynthesis pathway, triggers immune response against pathogens (Xu et al., 2018; Ullah et al., 2017). First line defence response activates after pathogen infection by rapid production of phenolic compounds (Yuan et al., 2019), provides indirect resistance to the plant (Ma et al., 2018). A study of Petkovsek et al. (2011) confirmed that phenolic metabolites restrict the pathogenic infection in cell wall of plants by inactivating fungal enzymes. In AS infected plants, *A. solani* induced the plant immune system, which might also induce phenylpropanoid pathway, resulting higher content of phenolic compounds. Previously, Asselbergh et al. (2007) reported that, reactive oxygen species (ROS) generated during pathogenic infection, to strengthen the plant defense system against *Botrytis cinerea*.

PAL activity was increased in AS alone (28.27 µmoles of TCA/mg of protein) after 72 h of post infection (Fig. 6d), whereas decreased level of PAL activity was recorded in PNE treated AS infected plants (23.33 µmoles of TCA/mg of protein). Moreover, the PAL content was higher in carbendazim treated plants (29.11 µmoles of TCA/mg of protein) in comparison to pathogen infected plants (Fig. 6d). The PAL content is a primary enzyme of phenylpropanoid pathway for phenolic compound synthesis (Tower and Wat, 1979), Tian et al., 2006 also observed the similar results of enhanced PAL activity during infection of *Alternria alternata*, to reduce the infection in *Pyrus pyrifolia*. In conclusion, the level of phenolic, PAL activity were higher in pathogen infected plants, and PNE decreased the enzymatic activity during *Alternaria* infection.

3.6. Effect of PNE on plant physiology during Alternaria solani infection

In order to elucidate the effect of PNE on plant physiology. Stomatal conductance, photosynthesis rate, transpiration rate and WUE were observed. Stomatal deregulation was noticed in AS infected plants by evaluation of stomatal conductance rate as compared with control. The stomatal conductance in control plants 0.827 mol m^{-2} s^{-1}while 0.361 mol m^{-2} s^{-1} in AS alone plants were measured. Conductance rate was not significantly different with AS + PNE and AS + Carb (0.424 and 0.394 mol m^{-2} s^{-1} respectively) during day time (Fig. 8 a). Transpiration and photosynthesis rate were measured in control plants (7.708 mmol m^{-2} s^{-1} and 26.5 µmol m^{-2} s^{-1} respectively), while in infected plants, rate was decreased in comparison to control plants (3.59 mmol m^{-2} s^{-1} and 25.32 µmol m^{-2} s^{-1}) (Fig8 c, b). Moreover, transpiration rate was increased in PNE treated pathogen infected plants by 5.06 mmol m^{-2} s^{-1}in comparison to AS + Carb (4.35 mmol m^{-2} s^{-1}) and AS alone (3.594 mmol m^{-2} s^{-1}) (Fig. 8c). Although, photosynthesis rate was also affected in presence of PNE (29.32 µmol m^{-2} s^{-1}) but it was not significantly distinct with AS + Carb (29.93 µmol m^{-2} s^{-1}) (Fig. 8b). PNE has ability to ameliorate the biotic stress condition by significantly enhancing photosynthesis and transpiration rate. Moreover, WUE was high in AS and AS + Carb (7.25 and 7.27 mol of CO_2 mol-1 of H_2O) than other treatments, and PNE pathogenic plant lower the WUE (5.97 mol of CO_2 mol-1 of H_2O), but it was not significantly different than pathogenic plant (Fig. 8d). Leaf and stomata morphology also corroborated with leaf physiology. An anomaly was observed in stomata of AS treated leaves by swollen guard cell with high number of fungal spores present on surface of leaf (Fig. 7), whereas stomatal morphology of AS + PNE was similar as control and less no of spores were observed (Fig. 7). Although, in AS + Carb, less number of spores and reduced stomatal analogy was observed, but a deposition of fungicide at stomatal opening was observed this may be the cause of less physiological activity (Fig. 7). Mishra et al. (2018) also advocated similar findings that pathogen infected plants reduced the physiological attributes during foliar infection

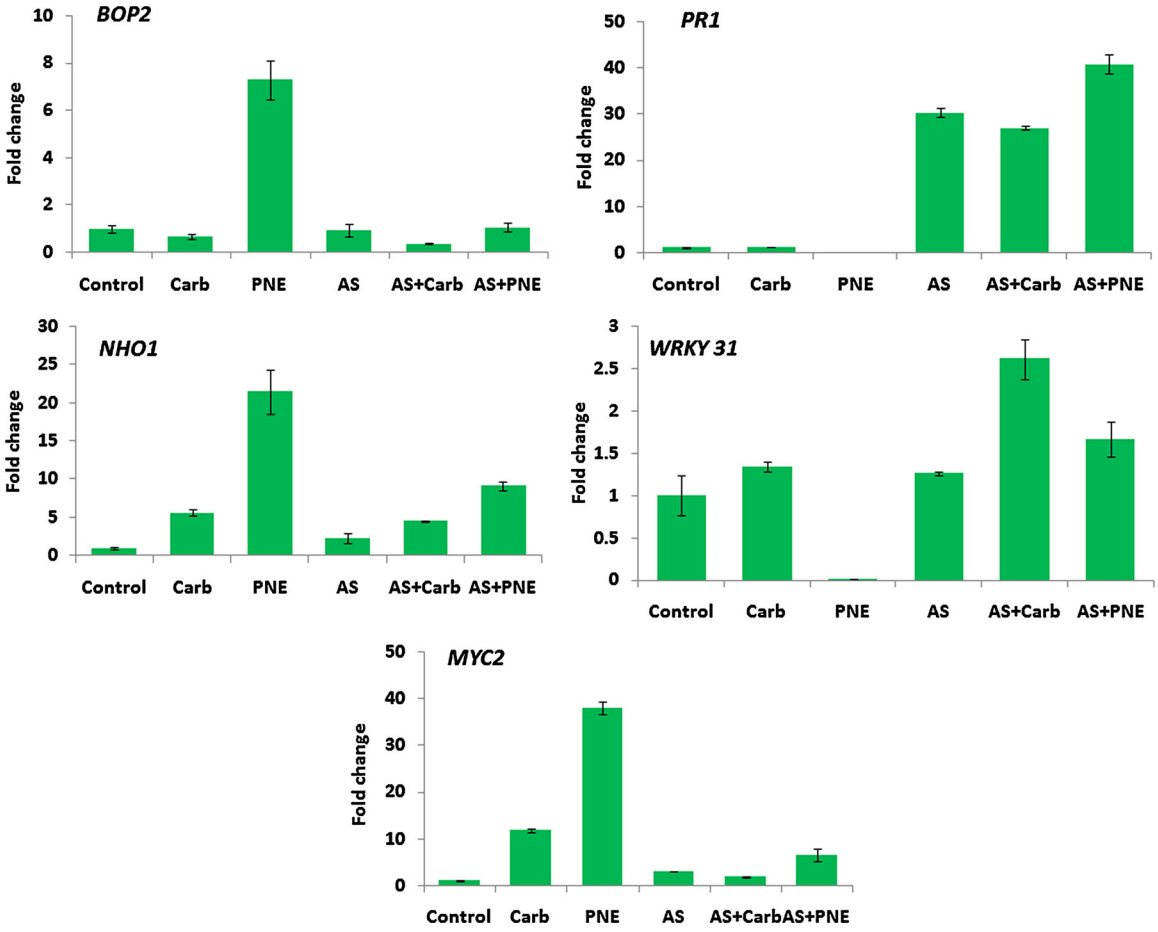

Fig. 9. Changes at gene expression level during interaction of tomato with different treatments: Control, Carb, PNE, AS, AS + Carb and AS + PNE. Expression levels were expressed in fold changes in comparison to control.

of *Alternaria alternata* in *Withania somnifera*. During the course of infection, fungal spores firstly attach on hydrophobic cuticlar surface of leaf (Hoefle and Hückelhoven, 2008), thereafter spores germinates in favorable condition (Łaźniewska et al., 2012). A large set of reactions happens from fungal penetration into the cell and plant respond against them. A necrophytic fungus adapt various strategies to penetrate and initiate the infection viz: formation of germ tube for penetration and producing cell wall degrading enzymes to digests cell wall components (Łaźniewska et al., 2012) also secreting toxins which hampers the ABA mediated stomatal closure mechanism and leading to stomata opening (Guimaraes and Stotz, 2004; Ton et al., 2009). In other reports, stomatal deregulation was observed after accumulation of sugar in guard cell in infected stomata (Farrell et al., 1969). Wang et al. (2015), also suggested that during foliar infection physiology of leaf became disturbed with slow rate photosynthesis, transpiration and stomatal conductance.

3.7. Gene expression analysis

All the findings of PNE as potential antifungal agent against *A. solani* in tomato, were further validated by gene expression analysis. The expression level of defense responsive genes: *BOP2, PR1, WRKY 31* were up-regulated by 1.06, 40.85 and 1.66 fold in PNE treated pathogen infected plants in comparison to control (Fig. 9). However, expression level of *MYC2* and *NHO1* was higher by 6.60 and 9.14 fold in AS + PNE compared to control (Fig. 9). The *MYC2* (jasmonic acid) and *SA* (*PR1*) are pathway specific defense responsive gene, they establish the cross talk between SA or JA/ethylene mediated pathways. In present study, a higher expression level of *PR1* than *MYC2* indicated to the SA dependent pathway according to Norman-Setterblad et al. (2000). *BOP2* is paralog of *NPR1* (Castelló et al., 2018), by over-expression of *BOP2* gene responsible for resistance by inducing methyl-jasmonate pathway supported by the previous study. Arabidopsis *NPR1* has been reported for enhanced resistance in variety of crop during biotrophic and necrotrophic infection (Cao et al., 1998; Kumar et al., 2013; Molla et al., 2016). *NPR1* is master regulator of systemic & acquired resistance (SAR) and induced systemic resistance (ISR) (Pieterse et al., 1998) by regulating the salicylic and jasmonic acid pathway (Backer et al., 2019). The PR gene initiate the systemic acquired resistance (SAR) (Balderas-Hernández et al., 2013; Backer et al., 2019). Our results well corroborated with the previous studies, over-expression of *NPR1* gene in PNE and AS + PNE treated plants, responsible for over-expression of *PR1* genes which was maximum in PNE treated pathogen infected plants than AS + Carb and AS alone. A reduced expression of *PR* genes was observed in *NPR1* deficient mutant plant, become more susceptible for pathogen attack (Cao et al., 1998; Roetschi et al., 2001). An over-expression of non-host resistance (*NHO*) gene also provides resistance in PNE and PNE + AS treatment. A study of Lu et al., 2001 also suggested the generic resistance in plant provided by *NHO1* gene in *Arabidopsis*. During infection of *A. solani*, a necrophytic fungus induced hypersensitive responses by activating *WRKY*, and *MYC2* genes to prevent further exposure (Adachi et al., 2016). *WRKY* gene is highly responsible for plant defense response against necrophytic fungus (Adachi et al., 2016). PNE was able to induce hypersensitive response against pathogen to restrict the infection of *A. solani.* All the finding and previous study demonstrated that PNE was able to induce more SA mediated systemic acquired resistance than jasmonic pathway response to restrict infection of *A. solani* and manage early blight disease in

tomato.

4. Conclusion

An eco-friendly nano-technological approach has been adopted to fulfill the objective for control the *A. solani* infection, a major causative agent of early bight disease in tomato. Peppermint oil based nanoemulsion, having size below to the 100 nm, with negative charges was synthesized. One percent of PNE was effective to inhibit the growth of *A. solani*, further proceeded for greenhouse study. Reduced number of *A. solani* spores in AS + PNE after 14 and 21 days clearly indicated the inhibitory action of PNE in sustainable manner. Plant triggered first line immune system by enhancing PAL activity to produce phenolic content which was further confirmed by profiling of gene expression with up-regulation of plant defence related gene in AS + PNE. Higher photosynthesis and transpiration rate in AS + PNE revealed the stress amelioration efficacy of PNE. Furthermore, chemical fungicide, carbendazim also controlled the fungal growth but it was not as efficient near to PNE. In conclusion of all the findings, PNE revealed as a promising formulation in future to combat early blight disease in an eco-friendly and cost-effective manner to promote sustainable agriculture.

CRediT authorship contribution statement

Shipra Pandey: Data curation, Formal analysis, Methodology, Writing - original draft, Writing - review & editing. **Ved Prakash Giri:** Data curation, Methodology, Writing - original draft. **Ashutosh Tripathi:** Data curation, Formal analysis, Methodology. **Madhuree Kumari:** Data curation, Writing - review & editing. **Shiv Narayan:** Data curation, Methodology. **Arpita Bhattacharya:** Formal analysis, Writing - review & editing. **Suchi Srivastava:** Writing - review & editing. **Aradhana Mishra:** Conceptualization, Funding acquisition, Investigation, Supervision, Project administration.

Declaration of Competing Interest

The authors declare that they have no conflict of interest.

Acknowledgments

This study was partially funded by 'Department of Science & Technology project' "GAP-3428. Authors thank to Director of CSIR-National Botanical Research Institute (NBRI), India for his necessary support. SP thanks to CSIR for awarding Senior Research Fellowship. Authors would like to thank Nidhi Arjaria for TEM analysis at Central Instrumentation Facility, CSIR- Indian Institute of Toxicology Research. Authors would also thank to Dr. Sandip Kumar Behera for SEM analysis at Central Instrumentation Facility, CSIR- NBRI, India.

Appendix A. Supplementary data

Supplementary material related to this article can be found, in the online version, at doi:https://doi.org/10.1016/j.indcrop.2020.112421.

References

Adachi, H., Ishihama, N., Nakano, T., Yoshioka, M., Yoshioka, H., 2016. *Nicotiana benthamiana* MAPK-WRKY pathway confers resistance to a necrotrophic pathogen *Botrytis cinerea*. Plant signaling & behavior 11 (6), e1183085. https://doi.org/10.1080/15592324.2016.1183085.

Adhikari, P., Oh, Y., Panthee, D., 2017. Current status of early blight resistance in tomato: an update. International journal of molecular sciences 18 (10), 2019. https://doi.org/10.3390/ijms18102019.

Araújo, G.M.F., Barros, A.R., Oshiro-Junior, J.A., Soares, L.F., da Rocha, L.G., de Lima, Á.A.N., da Silva, J.A., Converti, A., Damasceno, B.P.G.D.L., 2019. Nanoemulsions loaded with amphotericin B: development, characterization and leishmanicidal Activity. Current pharmaceutical design 25 (14), 1616–1622. https://doi.org/10.2174/1381612825666190705202030.

Arnon, D.I., 1949. Copper enzymes in isolated chloroplasts. Polyphenol oxidase in *Beta vulgaris*. Plant physiology 24 (1), 1. https://doi.org/10.1104/pp.24.1.1.

Asselbergh, B., Curvers, K., França, S.C., Audenaert, K., Vuylsteke, M., Van Breusegem, F., Höfte, M., 2007. Resistance to *Botrytis cinerea* in sitiens, an abscisic acid-deficient tomato mutant, involves timely production of hydrogen peroxide and cell wall modifications in the epidermis. Plant Physiology 144 (4), 1863–1877. https://doi.org/10.1104/pp.107.099226.

Aswani, V., Rajsheel, P., Bapatla, R.B., Sunil, B., Raghavendra, A.S., 2019. Oxidative stress induced in chloroplasts or mitochondria promotes proline accumulation in leaves of pea (*Pisumsativum*): another example of chloroplast-mitochondria interactions. Protoplasma 256 (2), 449–457. https://doi.org/10.1007/s00709-018-1306-1.

Backer, R., Naidoo, S., van den Berg, N., 2019. The NONEXPRESSOR OF PATHOGENESIS-RELATED GENES 1 (NPR1) and Related Family: Mechanistic Insights in Plant Disease Resistance. Frontiers in plant science 10. https://doi.org/10.3389/fpls.2019.00102.

Balderas-Hernández, V.E., Alvarado-Rodríguez, M., Fraire-Velázquez, S., 2013. Conserved versatile master regulators in signalling pathways in response to stress in plants. AoB Plants. https://doi.org/10.1093/aobpla/plt033.

Bates, L., Waldren, R.P., Teare, I.D., 1973. Rapid determination of free proline for water-stress studies. Plant and Soil 39, 205–207. https://doi.org/10.1007/BF00018060.

Cao, H., Li, X., Dong, X., 1998. Generation of broad-spectrum disease resistance by overexpression of an essential regulatory gene in systemic acquired resistance. Proceedings of the National Academy of Sciences 95 (11), 6531–6536. https://doi.org/10.1073/pnas.95.11.6531.

Castelló, M.J., Medina-Puche, L., Lamilla, J., Tornero, P., 2018. NPR1 paralogs of Arabidopsis and their role in salicylic acid perception. PloS one 13 (12).

Chhipa, H., 2017. Nanofertilizers and nanopesticides for agriculture. Environmental chemistry letters 15 (1), 15–22. https://doi.org/10.1007/s10311-016-0600-4.

Dallagnol, L.J., Rodrigues, F.A., Martins, S.C., Cavatte, P.C., DaMatta, F.M., 2011. Alterations on rice leaf physiology during infection by *Bipolaris oryzae*. Autralasian Plant Pathology 40 (4), 360–365. https://doi.org/10.1007/s13313-011-0048-8.

Dixit, R., Agrawal, L., Gupta, S., Kumar, M., Yadav, S., Chauhan, P.S., Nautiyal, C.S., 2016. Southern blight disease of tomato control by 1-aminocyclopropane-1-carboxylate (ACC) deaminase producing *Paenibacilluslentimorbus*B-30488. Plant signaling & behavior 11 (2), e1113363. https://doi.org/10.1080/15592324.2015.1113363.

Espitia, P.J., Fuenmayor, C.A., Otoni, C.G., 2019. Nanoemulsions: Synthesis, characterization, and application in bio-based active food packaging. Comprehensive Reviews in Food Science and Food Safety 18 (1), 264–285. https://doi.org/10.1111/1541-4337.12405.

Farrell, G.M., Preece, T.F., Wren, M.J., 1969. Effects of infection by *Phytophthora injestans* (Mont.) de Bary on the stomata of potato leaves. Annals of Applied Biology 63 (2), 265–275. https://doi.org/10.1111/j.1744-7348.1969.tb05488.x.

Garnault, M., Duplaix, C., Leroux, P., Couleaud, G., Carpentier, F., David, O., Walker, A.S., 2019. Spatiotemporal dynamics of fungicide resistance in the wheat pathogen *Zymoseptoria tritici* in France. Pest management science. https://doi.org/10.1002/ps.5360.

Guerra-Rosas, M.I., Morales-Castro, J., Ochoa-Martínez, L.A., Salvia-Trujillo, L., Martín-Belloso, O., 2016. Long-term stability of food-grade nanoemulsions from high methoxyl pectin containing essential oils. Food Hydrocolloids 52, 438–446. https://doi.org/10.1016/j.foodhyd.2015.07.017.

Guimaraes, R.L., Stotz, H.U., 2004. Oxalate production by *Sclerotinia sclerotiorum* deregulates guard cells during infection. Plant physiology 136 (3), 3703–3711. https://doi.org/10.1104/pp.104.049650.

Gundewadi, G., Sarkar, D.J., Rudra, S.G., Singh, D., 2018. Preparation of basil oil nanoemulsion using *Sapindus mukorossi* pericarp extract: Physico-chemical properties and antifungal activity against food spoilage pathogens. Industrial Crops and Products 125, 95–104. https://doi.org/10.1016/j.indcrop.2018.08.076.

Hashem, A.S., Awadalla, S.S., Zayed, G.M., Maggi, F., Benelli, G., 2018. *Pimpinella anisum* essential oil nanoemulsions against *Tribolium castaneum*—insecticidal activity and mode of action. Environmental Science and Pollution Research 25 (19), 18802–18812. https://doi.org/10.1007/s11356-018-2068-1.

Heath, R.L., Packer, L., 1968. Photoperoxidation in isolated chloroplasts: I. Kinetics and stoichiometry of fatty acid peroxidation. Archives of biochemistry and biophysics 125 (1), 189–198. https://doi.org/10.1016/0003-9861(68)90654-1.

Hoefle, C., Hückelhoven, R., 2008. Enemy at the gates: traffic at the plant cell pathogen interface. Cellular microbiology 10 (12), 2400–2407. https://doi.org/10.1111/j.1462-5822.2008.01238.x.

Jain, M., Mathur, G., Koul, S., Sarin, N., 2001. Ameliorative effects of proline on salt stress-induced lipid peroxidation in cell lines of groundnut (*Arachis hypogaea L.*). Plant Cell Reports 20 (5), 463–468. https://doi.org/10.1007/s002990100353.

Jaleel, C.A., Riadh, K., Gopi, R., Manivannan, P., Ines, J., Al-Juburi, H.J., Chang-Xing, Z., Hong-Bo, S., Panneerselvam, R., 2009. Antioxidant defense responses: physiological plasticity in higher plants under abiotic constraints. Acta Physiologiae Plantarum 31 (3), 427–436. https://doi.org/10.1007/s11738-009-0275-6.

Khan, I.A., Abourashed, E.A., 2011. Leung's encyclopedia of common natural ingredients: used in food, drugs and cosmetics. John Wiley Sons.

Kumar, V., Joshi, S.G., Bell, A.A., Rathore, K.S., 2013. Enhanced resistance against *Thielaviopsis basicola* in transgenic cotton plants expressing Arabidopsis NPR1 gene. Transgenic research 22 (2), 359–368. https://doi.org/10.1007/s11248-012-9652-9.

Kumari, M., Pandey, S., Bhattacharya, A., Mishra, A., Nautiyal, C.S., 2017a. Protective role of biosynthesized silver nanoparticles against early blight disease in *Solanum lycopersicum*. Plant physiology and biochemistry 121, 216–225. https://doi.org/10.1016/j.plaphy.2017.11.004.

Kumari, M., Shukla, S., Pandey, S., Giri, V.P., Bhatia, A., Tripathi, T., Kakkar, P., Nautiyal, C.S., Mishra, A., 2017b. Enhanced cellular internalization: a bactericidal mechanism more relative to biogenic nanoparticles than chemical counterparts. ACS applied materials & interfaces 9 (5), 4519–4533. https://doi.org/10.1021/acsami.6b15473.

Łaźniewska, J., Macioszek, V.K., Kononowicz, A.K., 2012. Plant-fungus interface: the role of surface structures in plant resistance and susceptibility to pathogenic fungi. Physiological and Molecular Plant Pathology 78, 24–30. https://doi.org/10.1016/j.pmpp.2012.01.004.

Liang, R., Xu, S., Shoemaker, C.F., Li, Y., Zhong, F., Huang, Q., 2012. Physical and antimicrobial properties of peppermint oil nanoemulsions. Journal of agricultural and food chemistry 60 (30), 7548–7555. https://doi.org/10.1021/jf301129k.

Lim, H.W., Kim, H., Kim, J., Bae, D., Song, K.Y., Chon, J.W., Lee, J.M., Kim, S.H., Kim, D.H., Seo, K.H., 2018. Antimicrobial effect of *Mentha piperita* (peppermint) oil against *Bacillus cereus*, *Staphylococcus aureus*, *Cronobacter sakazakii*, and *Salmonella Enteritidis* in various dairy foods: Preliminary study. Journal of Milk Science and Biotechnology 36 (3), 146–154. https://doi.org/10.22424/jmsb.2018.36.3.146.

Livak, K.J., Schmittgen, T.D., 2001. Analysis of relative gene expression data using real-time quantitative PCR and the $2^{-\Delta\Delta CT}$ method. methods 25 (4), 402–408 10.1006/meth.2001.1262.

Lopisso, D.T., Knüfer, J., Koopmann, B., von Tiedemann, A., 2017. The vascular pathogen *Verticillium longisporum* does not affect water relations and plant responses to drought stress of its host, *Brassica napus*. Phytopathology 107 (4), 444–454. https://doi.org/10.1094/PHYTO-07-16-0280-R.

Louni, M., Shakarami, J., Negahban, M., 2018. Insecticidal efficacy of nanoemulsion containing *Mentha longifolia* essential oil against *Ephestia kuehniella* (Lepidoptera: Pyralidae). Journal of Crop Protection 7 (2), 171–182.

Lu, M., Tang, X., Zhou, J.M., 2001. Arabidopsis *NHO1* is required for general resistance against Pseudomonas bacteria. The Plant Cell 13 (2), 437–447. https://doi.org/10.1105/tpc.13.2.437.

Lubaina, A.S., Murugan, K., 2013. Ultrastructural changes and oxidative stress markers in wild and cultivar Sesamum orientale L. following Alternaria sesami (Kawamura) Mohanty and Behera. Inoculation. http://nopr.niscair.res.in/handle/123456789/20480.

Ma, L., He, J., Liu, H., Zhou, H., 2018. The phenylpropanoid pathway affects apple fruit resistance to *Botrytis cinerea*. Journal of Phytopathology 166 (3), 206–215. https://doi.org/10.1111/jph.12677.

Mahboubi, M., Kazempour, N., 2014. Chemical composition and antimicrobial activity of peppermint (*Mentha piperita* L.) Essential oil. Songklanakarin J. Sci. Technol 36 (1), 83–87.

McClements, D.J., 2011. Edible nanoemulsions: fabrication, properties, and functional performance. Soft Matter 7 (6), 2297–2316. https://doi.org/10.1039/C0SM00549E.

Meena, M., Zehra, A., Dubey, M.K., Aamir, M., Gupta, V.K., Upadhyay, R.S., 2016. Comparative evaluation of biochemical changes in tomato (*Lycopersicon esculentum* Mill.) infected by *Alternaria alternata* and its toxic metabolites (TeA, AOH, and AME). Frontiers in plant science 7, 1408. https://doi.org/10.3389/fpls.2016.01408.

Mishra, A., Singh, S.P., Mahfooz, S., Singh, S.P., Bhattacharya, A., Mishra, N., Nautiyal, C.S., 2018. Endophyte-mediated modulation of defense-related genes and systemic resistance in *Withania somnifera* (L.) Dunal under *Alternaria alternata* stress. Appl. Environ. Microbiol. 84 (8), e02845–17. https://doi.org/10.1128/AEM.02845-17.

Molla, K.A., Karmakar, S., Chanda, P.K., Sarkar, S.N., Datta, S.K., Datta, K., 2016. Tissue-specific expression of Arabidopsis *NPR1* gene in rice for sheath blight resistance without compromising phenotypic cost. Plant Science 250, 105–114. https://doi.org/10.1016/j.plantsci.2016.06.005.

Nam, Y.S., Kim, J.W., Park, J., Shim, J., Lee, J.S., Han, S.H., 2012. Tocopheryl acetate nanoemulsions stabilized with lipid–polymer hybrid emulsifiers for effective skin delivery. Colloids and Surfaces B: Biointerfaces 94, 51–57. https://doi.org/10.1016/j.colsurfb.2012.01.016.

Nicoletto, C., Maucieri, C., Zanin, G., Vianello, F., Sambo, P., 2019. Vegetables Quality and Biotic Stress. Plant Health under Biotic Stress 107-128. Springer, Singapore. https://doi.org/10.1007/978-981-13-6043-5_6.

Norman-Setterblad, C., Vidal, S., Palva, E.T., 2000. Interacting signal pathways control defense gene expression in Arabidopsis in response to cell wall-degrading enzymes from *Erwinia carotovora*. Molecular Plant-Microbe Interactions 13 (4), 430–438. https://doi.org/10.1094/MPMI.2000.13.4.430.

Oerke, E.C., 2006. Crop losses to pests. The Journal of Agricultural Science 144 (1), 31–43. https://doi.org/10.1017/S0021859605005708.

Ostertag, F., Weiss, J., McClements, D.J., 2012. Low-energy formation of edible nanoemulsions: factors influencing droplet size produced by emulsion phase inversion. Journal of colloid and interface science 388 (1), 95–102. https://doi.org/10.1016/j.jcis.2012.07.089.

Petkovsek, M.M., Slatnar, A., Stampar, F., Veberic, R., 2011. Phenolic compounds in apple leaves after infection with apple scab. Biologia plantarum 55 (4), 725. https://doi.org/10.1007/s10535-011-0176-6.

Pétriacq, P., Stassen, J.H., Ton, J., 2016. Spore density determines infection strategy by the plant pathogenic fungus *Plectosphaerella cucumerina*. Plant Physiology 170 (4), 2325–2339. https://doi.org/10.1104/pp.15.00551.

Pieterse, C.M., Van Wees, S.C., Van Pelt, J.A., Knoester, M., Laan, R., Gerrits, H., Weisbeek, P.J., Van Loon, L.C., 1998. A novel signaling pathway controlling induced systemic resistance in Arabidopsis. The Plant Cell 10 (9), 1571–1580. https://doi.org/10.1105/tpc.10.9.1571.

Polyakov, A.Y., Lebedev, V.A., Volkov, D.S., Pankratov, D.A., Veligzhanin, A.A., Perminova, I.V., Lucena, J.J., 2019. Eco-friendly iron-humic nanofertilizers synthesis for the prevention of iron chlorosis in soybean (*Glycine max*) grown in calcareous soil. Frontiers in plant science 10, 413. https://doi.org/10.3389/fpls.2019.00413.

Priester, J.H., Ge, Y., Mielke, R.E., Horst, A.M., Moritz, S.C., Espinosa, K., Gelb, J., Walker, S.L., Nisbet, R.M., An, Y.J., Schimel, J.P., 2012. Soybean susceptibility to manufactured nanomaterials with evidence for food quality and soil fertility interruption. Proceedings of the National Academy of Sciences 109 (37), E2451–E2456. https://doi.org/10.1073/pnas.1205431109.

Raliya, R., Saharan, V., Dimkpa, C., Biswas, P., 2017. Nanofertilizer for precision and sustainable agriculture: current state and future perspectives. Journal of agricultural and food chemistry 66 (26), 6487–6503. https://doi.org/10.1021/acs.jafc.7b02178.

Roetschi, A., Si-Ammour, A., Belbahri, L., Mauch, F., Mauch-Mani, B., 2001. Characterization of an Arabidopsis–*Phytophthora pathosystem*: resistance requires a functional PAD2 gene and is independent of salicylic acid, ethylene and jasmonic acid signalling. The Plant Journal 28 (3), 293–305. https://doi.org/10.1046/j.1365-313X.2001.01148.x.

Saberi, A.H., Fang, Y., McClements, D.J., 2013. Fabrication of vitamin E-enriched nanoemulsions: factors affecting particle size using spontaneous emulsification. Journal of colloid and interface science 391, 95–102. https://doi.org/10.1016/j.jcis.2012.08.069.

Sharma, A., Sharma, N.K., Srivastava, A., Kataria, A., Dubey, S., Sharma, S., Kundu, B., 2018. Clove and lemongrass oil based non-ionic nanoemulsion for suppressing the growth of plant pathogenic *Fusarium oxysporum* f. sp. *lycopersici*. Industrial crops and products 123, 353–362. https://doi.org/10.1016/j.indcrop.2018.06.077.

Silva, A.P., Nunes, B.R., De Oliveira, M.C., Koester, L.S., Mayorga, P., Bassani, V.L., Teixeira, H.F., 2009. Development of topical nanoemulsions containing the isoflavonegenistein. Die Pharmazie-An International Journal of Pharmaceutical Sciences 64 (1), 32–35. https://doi.org/10.1691/ph.2009.8150.

Singh, A., Sarma, B.K., Upadhyay, R.S., Singh, H.B., 2013. Compatible rhizosphere microbes mediated alleviation of biotic stress in chickpea through enhanced antioxidant and phenylpropanoid activities. Microbiological Research 168 (1), 33–40. https://doi.org/10.1016/j.micres.2012.07.001.

Sugumar, S., Clarke, S.K., Nirmala, M.J., Tyagi, B.K., Mukherjee, A., Chandrasekaran, N., 2014. Nanoemulsion of eucalyptus oil and its larvicidal activity against *Culex quinquefasciatus*. Bulletin of entomological research 104 (3), 393–402. https://doi.org/10.1017/S0007485313000710.

Tian, S., Wan, Y., Qin, G., Xu, Y., 2006. Induction of defense responses against *Alternaria* rot by different elicitors in harvested pear fruit. Applied Microbiology and Biotechnology 70 (6). https://doi.org/10.1007/s00253-005-0125-4. 729.

Tiwari, S.K., Agarwal, S., Seth, B., Yadav, A., Nair, S., Bhatnagar, P., Karmakar, M., Kumari, M., Chauhan, L.K.S., Patel, D.K., Srivastava, V., 2014. Curcumin-loaded nanoparticles potently induce adult neurogenesis and reverse cognitive deficits in Alzheimer's disease model via canonical Wnt/β-catenin pathway. ACS nano 8 (1), 76–103. https://doi.org/10.1021/nn405077y.

Ton, J., Flors, V., Mauch-Mani, B., 2009. The multifaceted role of ABA in disease resistance. Trends in plant science 14 (6), 310–317. https://doi.org/10.1016/j.tplants.2009.03.006.

Tower, G.N., Wat, C.K., 1979. Phenylpropanoid metabolism. Planta Medica 37 (97-), 114. https://doi.org/10.1055/s-0028-1097309.

Ullah, C., Unsicker, S.B., Fellenberg, C., Constabel, C.P., Schmidt, A., Gershenzon, J., Hammerbacher, A., 2017. Flavan-3-ols are an effective chemical defense against rust infection. Plant physiology 175 (4), 1560–1578. https://doi.org/10.1104/pp.17.00842.

Van Tran, V., Nguyen, T.L., Moon, J.Y., Lee, Y.C., 2019. Core-shell materials, lipid particles and nanoemulsions, for delivery of active anti-oxidants in cosmetics applications: challenges and development strategies. Chemical Engineering Journal. https://doi.org/10.1016/j.cej.2019.02.168.

Vendruscolo, E.C.G., Schuster, I., Pileggi, M., Scapim, C.A., Molinari, H.B.C., Marur, C.J., Vieira, L.G.E., 2007. Stress-induced synthesis of proline confers tolerance to water deficit in transgenic wheat. Journal of plant physiology 164 (10), 1367–1376. https://doi.org/10.1016/j.jplph.2007.05.001.

Walia, N., Dasgupta, N., Ranjan, S., Chen, L., Ramalingam, C., 2017. Fish oil based vitamin D nanoencapsulation by ultrasonication and bioaccessibility analysis in simulated gastro-intestinal tract. Ultrasonics sonochemistry 39, 623–635. https://doi.org/10.1016/j.ultsonch.2017.05.021.

Walker, R., Decker, E.A., McClements, D.J., 2015. Development of food-grade nanoemulsions and emulsions for delivery of omega-3 fatty acids: opportunities and obstacles in the food industry. Food & function 6 (1), 41–54. https://doi.org/10.1039/C4FO00723A.

Wang, M., Sun, Y., Sun, G., Liu, X., Zhai, L., Shen, Q., Guo, S., 2015. Water balance altered in cucumber plants infected with *Fusarium oxysporum* f. sp. *cucumerinum*. Scientific reports 5, 7722. https://doi.org/10.1038/srep07722.

Weber, R.W., Hahn, M., 2019. Grey mould disease of strawberry in northern Germany: causal agents, fungicide resistance and management strategies. Applied microbiology and biotechnology 103 (4), 1589–1597. https://doi.org/10.1007/s00253-018-09590-1.

Xu, C., Cao, L., Zhao, P., Zhou, Z., Cao, C., Li, F., Huang, Q., 2018. Emulsion-based synchronous pesticide encapsulation and surface modification of mesoporous silica nanoparticles with carboxymethyl chitosan for controlled azoxystrobin release. Chemical Engineering Journal 348, 244–254. https://doi.org/10.1016/j.cej.2018.05.008.

Yuan, S., Ding, X., Zhang, Y., Cao, J., Jiang, W., 2019. Characterization of defense responses in the 'green ring' and 'red ring' on jujube fruit upon postharvest infection by *Alternaria alternata* and the activation by the elicitor treatment. Postharvest Biology and Technology 149, 166–176. https://doi.org/10.1016/j.postharvbio.2018.12.003.

Zhao, J., Li, S., Jiang, T., Liu, Z., Zhang, W., Jian, G., Qi, F., 2012. Chilling stress—the key predisposing factor for causing *Alternaria alternata* infection and leading to cotton (*Gossypium hirsutum L.*) leaf senescence. PLoS One 7 (4), e36126. https://doi.org/10.1371/journal.pone.0036126.